ChemComm

Accepted Manuscript

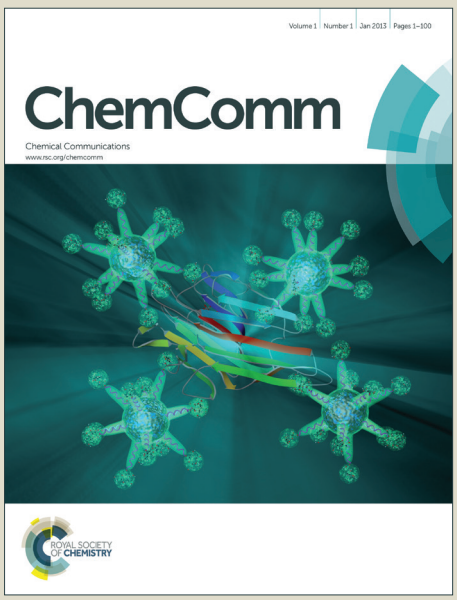

ROYAL SOCIETY OF CHEMISTRY

www.rsc.org/chemcomm

Journal Name

RSCPublishing

COMMUNICATION

Phase Transfer and Dispersion of Reduced Graphene Oxide Nanosheets Using Cluster Suprasurfactants

Cite this: DOI: 10.1039/x0xx00000x

Shan Wang, Haolong Li,* Liying Zhang, Bao Li, Xiao Cao, Guohua Zhang, Shilin Zhang and Lixin Wu*

Received 00th January 2012,
Accepted 00th January 2012

DOI: 10.1039/x0xx00000x

www.rsc.org/

Surfactant-encapsulated polyoxometalate complexes are used as cluster suprasurfactants to transfer reduced graphene oxide (RGO) nanosheets from water to low polar organic solvents, which realizes the single-layer dispersion and the cluster-functionalization of RGO in one step.

Graphene has attracted much attention in the last decade due to its excellent electronic, mechanical and thermal properties.[1] For the large scale production of graphene-based materials, a widely adopted strategy is using chemically exfoliated graphene oxide (GO) as a low cost precursor and converting it to reduced GO (RGO).[2] However, when targeting the process of RGO, two important issues need to be addressed: the dispersion and the functionalization of RGO.

Because of the strong intersheet adsorption, RGO have a tendency to form irreversible agglomerates and are only dispersible in polar media such as water and dimethylformamide (DMF), but not in low-polar solvents like chloroform and toluene.[2b] To disperse RGO in low-polar media, stabilizing groups are needed to be modified on the RGO. Alkyl chains and polymer groups have been grafted to RGO by covalent bond to improve their dispersion.[3] In comparison, the noncovalent modification of RGO, taking the advantage of avoiding complicated chemical processes, is recognized as a facile and alternative way to disperse RGO. In principle, the noncovalent dispersion of RGO is realized using the stabilizers that can interact with RGO by ionic bond,[4a,4b] π–π interaction,[4c] hydrophobic effect[4d] and so on. However, most of the stabilizers are organic and polymeric molecules whose structures rarely contain inorganic motifs. It is still a challenge to fabricate inorganically functionalized RGO with a high dispersibility in low-polar media.

Polyoxometalates (POMs) are nanoscale metal-oxide clusters with large compositional, structural and functional diversities.[5] Recent works reveals that POMs can strongly adsorb on graphene surface, leading to stable nanocomposites.[6] This finding indicates that the POM-graphene interaction may act as driving force to enable POMs to stabilize RGO in low-polar media, if suitable organic groups are modified on POMs. It has been reported that cationic surfactants can replace the counterions of POMs, forming surfactant-encapsulated POM complexes (SEPs) which have a typical amphiphilic structure and show surfactant-like properties,[7] for example, stabilizing water droplets.[7b,7c] It is reasonable to use SEPs to stabilize RGO through the POM-graphene interaction. In this context, we present a facile approach to fabricate organically dispersable cluster-functionalized RGO nanosheets, by using SEPs as cluster suprasurfactants to transfer RGO from water to chloroform, as shown in Scheme 1.

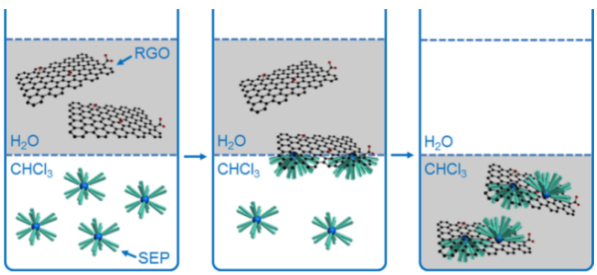

Scheme 1 The process of SEPs transferring RGO from water to chloroform.

GO nanosheets were prepared following a modified Hummers method (see detailed procedures in the ESI†).[8] Atomic force microscopy (AFM) images (Fig. S1) show that the size of GO is in the range from 200 to 400 nm, consistent with the dynamic light scattering (DLS) result (about 340 nm, Fig. S2), and the thickness is about 0.98 nm in accord with that of single-layer GO in the literature.[2a] After the reduction by hydrazine,[2a] the hydrodynamic diameter (D_h) of RGO nanosheets is about 300 nm (Fig. S3b), smaller than the initial GO, probably due to the shrinkage induced by the increased hydrophobicity; meanwhile, the zeta potential is –36 mV, revealing the RGO retain a high colloidal stability. Single-layer RGO nanosheets were observed on HOPG substrate by AFM (Fig. S4a). C1s X-ray photoelectron spectroscopy (XPS) result (Fig. S4b) shows that the content of oxygen-containing groups of GO decreases from initial 64.5% to 11.4% after reduction, indicating the efficient elimination of these groups in RGO (Table S1).

To obtain a systematic insight on how the structure of SEPs influences their abilities to phase transfer RGO, we synthesized a series of SEPs with a similar POM cluster part but gradually changed alkyl chain density on the surface of POMs, through using cationic surfactants dimethyldioctadecylammonium bromide (DODA·Br) to replace the counterions of seven Keggin-type POMs with charge numbers from 4 to 10. The formed SEPs are $(DODA)_4[SiW_{12}O_{40}]$ (SEP-4), $(DODA)_5[BW_{12}O_{40}]$ (SEP-5), $(DODA)_6[CoW_{12}O_{40}]$ (SEP-6), $(DODA)_7[PW_{11}O_{39}]$ (SEP-7),

$(DODA)_8[SiW_{11}O_{39}]$ (SEP-8), $(DODA)_9[BW_{11}O_{39}]$ (SEP-9), $(DODA)_{10}[SiW_9O_{34}]$ (SEP-10) (see detailed procedures and characterizations in the ESI†).

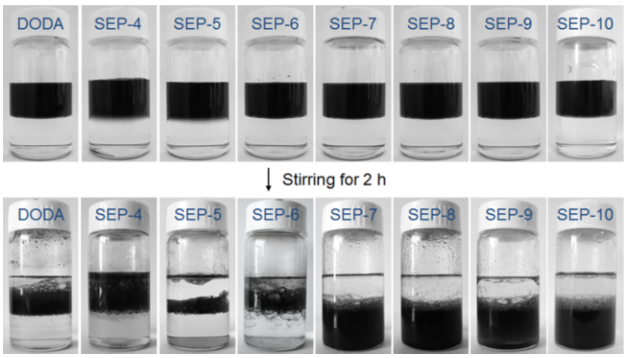

Fig. 1 Photographs of the phase transfer results. Parallel experiments were conducted using RGO (0.35 mg, 7 mL H_2O) and SEPs (4.5×10^{-7} mol, 7 mL chloroform) or DODA·Br (4.0×10^{-6} mol, 7 mL chloroform).

The maximum adsorption value of SEP-4 on RGO nanosheets is calculated to be 1.3×10^{-6} mol mg^{-1} (see detailed calculations in the ESI†). This value was used for all the seven SEPs as the condition to transfer RGO. The phase transfer phenomena are shown in Fig. 1. DODA·Br failed to transfer RGO, which should result from the neutral condition of RGO aqueous solution in our case. This result is consistent with literatures that GO or RGO can be transferred to chloroform by cationic surfactants only at pH value of 9.[4a,4b] The SEPs exhibit a gradually changed phase transfer ability depending on their DODA numbers. For SEP-4, SEP-5 and SEP-6, they failed to transfer RGO. When the DODA number was increased to 7, 8, 9 or 10, successful phase transfer occurs with 100% transfer efficiency as confirmed by the UV-vis-NIR spectra of water phase (Fig. S6). However, the stabilities of transferred RGO dispersions are different. For SEP-9/RGO and SEP-10/RGO, they precipitated from chloroform as black floccules after staying for 0.5 h (Fig. S7). However, SEP-7/RGO and SEP-8/RGO are very stable in chloroform after staying for 30 days (Fig. S7), and DLS results (Fig. S8 and S9) show that their D_h values are both about 350 nm. Moreover, the UV-vis-NIR spectra of both SEP-7/RGO and SEP-8/RGO in chloroform (Fig. S10) exhibit straight linear relationships between the absorbance at 800 nm and the concentration of RGO, well obeying the Beer's law, further demonstrating their good dispersibility.[9]

It has been reported that the hydrophobic and the hydrophilic parts of SEPs phase separate at water/oil interface, forming a asymmetric structure where the alkyl chains are toward organic phase while the POM clusters face to water phase.[7e] The phase separation of SEPs is assumed to play an important role during the phase transfer of RGO. It allows the POM clusters to be exposed and adsorb onto RGO nanosheets at the water/chloroform interface, and then the hydrophobic DODA chains pull RGO to chloroform. Based on this mechanism, two factors reasonably contribute to the phase transfer ability of SEPs: (i) the hydrophobicity of SEPs which directly affects the solubility of SEP/RGO in chloroform; (ii) the interacting area between POMs and RGO which influences the adsorption stability of SEPs on RGO and thus determines the stability of final SEP/RGO dispersion. To simplify the calculation, we used carbon atom density to represent the hydrophobicity of SEPs, which is obtained through dividing the carbon atom numbers by the surface area of POMs. The structure parameters of SEPs are summarized in Table 1. The surface areas of POMs as ideal spheres are all about 8.04 nm^2 on the basis of which their radius is 0.52 nm and their van der Waals radius is 0.28 nm.[10] As a DODA contains 38 carbon atoms, the carbon atom densities of SEPs are estimated to be 18.90, 23.63, 28.36, 33.08, 37.81, 42.54 and 47.26 nm^{-2}, respectively. The POM-RGO interacting area is calculated to be 1.16 nm^2 by using the detailed method in the Fig. S11. And the average DODA areas of SEPs adsorbed on RGO are calculated by using the surface area of POMs to subtract the POM-RGO interacting area, and then to divide the DODA numbers.

Table 1 Summary of the structure parameters of SEPs.

	SEP-4	SEP-5	SEP-6	SEP-7	SEP-8	SEP-9	SEP-10
DODA number	4	5	6	7	8	9	10
carbon atom number	152	190	228	266	304	342	380
carbon atom density / nm^{-2}	18.90	23.63	28.36	33.08	37.81	42.54	47.26
average DODA area of free SEPs /nm^2 [a]	2.01	1.61	1.34	1.15	1.00	0.89	0.80
average DODA area of adsorbed SEPs / nm^2 [b]	1.72	1.38	1.15	0.98	0.86	0.76	0.69

[a] The average occupying area of DODA on the surface of POMs in free SEPs. [b] The average occupying area of DODA on the surface of POMs in the SEPs adsorbed on RGO.

It was found that when the carbon atom density of SEP reaches 33.08 with a DODA number ≥ 7, the resulting hydrophobicity is large enough for the phase transfer of RGO. Then we discuss the relationship between the structure of SEPs and the stability of SEP/RGO dispersions. For SEP-7 and SEP-8, their average DODA areas after adsorbing on RGO are 0.98 and 0.86 nm^2, respectively, which corresponds to a relatively loose stacking state of DODA alkyl chains, since they are larger than the molecular area of DODA in solid-sate Langmuir monolayers that is about 0.75 nm^2.[7d] This condition can provide POM-7 and POM-8 enough surface area to strongly adsorb on RGO, leading to a stable dispersion. The $\nu_{as}(W{=}O_d)$ vibration bands of SEP-7 and SEP-8 appear at 950 and 947 cm^{-1} in IR spectra, while they shift to 941 and 936 cm^{-1} for SEP-7/RGO and SEP-8/RGO, respectively (Fig. S12b and S12c). These phenomena are similar to the cases of POMs adsorbed on graphene, indicative of the electron transfer interactions between POM clusters and RGO nanosheets.[11] XPS results (Fig. S14) show that the $W^{VI}4f_{5/2}$ and $W^{VI}4f_{7/2}$ signals of SEP-7/RGO shift to higher binding energies compared with those of SEP-7, suggesting that the d^1 electron in POM-7 becomes easier to delocalize[12] on RGO, which should result from the electron transfer between POM-7 and RGO.[11] However, the average DODA areas of adsorbed SEP-9 and SEP-10 are 0.76 and 0.69 nm^2, respectively, which are close to or smaller than the case of tightly stacked DODA in Langmuir monolayers under a high surface pressure.[7d] In these cases, SEP-9 and SEP-10 cannot remain the initial phase separation states when SEP-9/RGO and SEP-10/RGO transfer from the water/oil interface to chloroform, which weaken the interactions between POM-9 or POM-10 and RGO, subsequently causing the dissociation of SEP from RGO and the precipitation of SEP-9/RGO and SEP-10/RGO. As expected, SEP-9 and SEP-10 show no obvious IR changes in SEP-9/RGO and SEP-10/RGO precipitate (Fig. S12d and S12e), meaning destructed interactions. Therefore, the high hydrophobicity and stable adsorption of SEPs are both important factors to obtain a stable SEP/RGO dispersion.

SEP-7/RGO is chosen as the sample of well-dispersed SEP/RGO nanocomposite for further structure characterizations. When casting

the SEP-7/RGO dispersion on a copper grid, many single-layer nanosheets are observed under transmission electron microscopy (TEM) in Fig. 2a and Fig. S15, confirming its monodispersed state. Magnified TEM image (Fig. 2b) shows that black dots about 1 nm in diameter uniformly distributed on the nanosheets, which should be the POM-7 cluster part of SEP-7 confirmed by Energy-dispersive X-ray spectroscopy with the presence of tungsten (Fig. 2c). The TGA result shows the mass ratio between the adsorbed SEP-7 and RGO nanosheets is 3:5 (Fig. S16). Due to the adsorption of SEP-7, the RGO thickness obtained from AFM height profile is about 4.00 nm (Fig. 2d), obviously larger than that of unmodified RGO nanosheets which is normally 1 nm measured by AFM.[13] X-ray diffraction (XRD) patterns of RGO, SEP-7 and SEP-7/RGO are shown in Fig. 3a. The interlayer spacing of RGO is about 0.37 nm; while for SEP-7/RGO, it increases to 5.17 nm, indicating an intercalation effect arising from the adsorption of SEP-7, as seen in the proposed stacking model of SEP-7/RGO nanosheets in Fig 3b. The XRD pattern of pure SEP-7 exhibits an ordered lamellar structure with a spacing of 3.31 nm. The reported interacting distance between POMs and graphene is 0.25 nm,[11a] and the radius of POM-7 is 0.52 nm. According to the proposed stacking model, the interlayer spacing of two adjacent RGO nanosheets in SEP-7/RGO can be calculated using 0.37 + (0.25 + 0.52) × 2 + 3.31, which gives a sum of 5.21 nm, well consistent with the experimental value of 5.17 nm. These results indicate that the SEP-dispersed RGO nanosheets are promising precursors for the preparation of graphene-cluster intercalation nanocomposites.

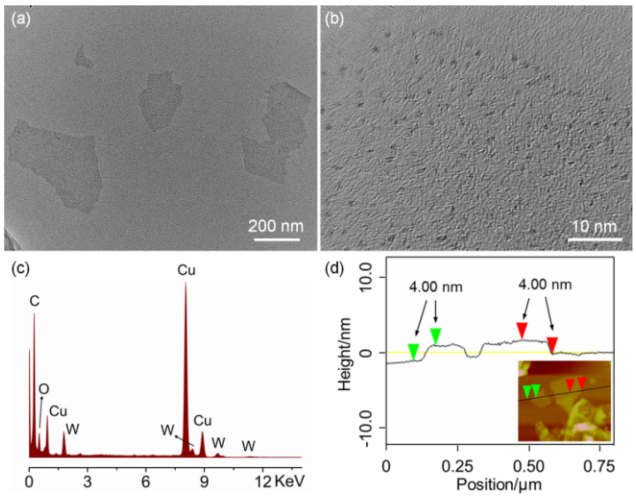

Fig. 2 (a) and (b) TEM images of SEP-7/RGO. (c) The corresponding EDX spectra of (b). (c) The height profile of AFM image (inset) of SEP-7/RGO on HOPG substrate.

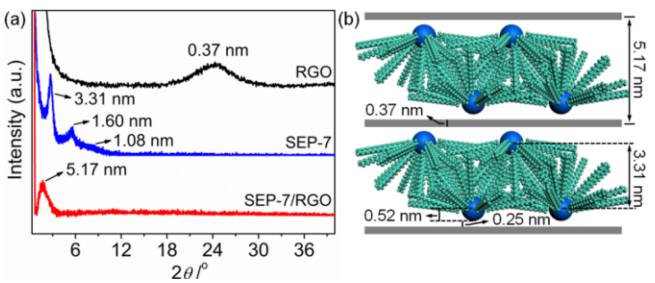

Fig. 3 (a) XRD patterns of powder RGO (black), casting SEP-7 (blue) and SEP-7/RGO nanocomposite (red) in chloroform solutions. (b) The possible stacking model of SEP-7/RGO nanosheets.

Conclusions

SEPs can act as cluster suprasurfactants to transfer RGO from water to low polar media, realizing efficient organic dispersion of RGO nanosheets as single layers. The mechanism is based on the strong adsorption between the POM cluster cores inside SEPs and the RGO nanosheets. This finding not only provides a new approach to disperse RGO but also realizes the modification of RGO with inorganic clusters simultaneously, which is instructive for fabricating functional graphene nanocomposites. The study of the synergy properties (e.g. catalysis) of POMs and RGO in these nanocomposites is ongoing in our lab.

This work is financially supported by the financial supports from the National Natural Science Foundation of China (51102112, 20921003) and Jilin Provincial Science & Technology Department (201201013).

Notes and references

State Key Laboratory of Supramolecular Structure and Materials, College of Chemistry, Jilin University, Changchun 130012, China
E-mail: hl_li@jlu.edu.cn; wulx@jlu.edu.cn

† Electronic Supplementary Information (ESI) available: experimental details, characterizations of the SEP/RGO, calculation of POM-RGO interacting area. See DOI: 10.1039/c000000x/

1 A. K. Geim and K. S. Novoselov, *Nat. Mater.*, 2007, **6**, 183.
2 (a) S. Stankovich, D. A. Dikin, R. D. Piner, K. A. Kohlhaas, A. Kleinhammes, Y. Jia, Y. Wu, S. T. Nguyen and R. S. Ruoff, *Carbon*, 2007, **45**, 1558; (b) D. R. Dreyer, S. Park, C. W. Bielawski and R. S. Ruoff, *Chem. Soc. Rev.*, 2010, **39**, 228.
3 (a) S. Niyogi, E. Bekyarova, M. E. Itkis, J. L. McWilliams, M. A. Hamon and R. C. Haddon, *J. Am. Chem. Soc.*, 2006, **128**, 7720; (b) Y. S. Ye, Y. N. Chen, J. S. Wang, J. Rick, Y. J. Huang, F. C. Chang and B. J. Hwang, *Chem. Mater.*, 2012, **24**, 2987.
4 (a) Y. Liang, D. Wu, X. Feng and K. Müllen, *Adv. Mater.*, 2009, **21**, 1679; (b) S. Yin, Y. Zhang, J. Kong, C. Zou, C. M. Li, X. Lu, J. Ma, F. Y. C. Boey and X. Chen, *ACS Nano*, 2011, **5**, 3831; (c) F. Li, Y. Bao, J. Chai, Q. Zhang, D. Han and L. Niu, *Langmuir*, 2010, **26**, 12314; (d) T. Wei, G. Luo, Z. Fan, C. Zheng, J. Yan, C. Yao, W. Li and C. Zhang, *Carbon*, 2009, **47**, 2290.
5 (a) M. T. Pope and A. Müller, *Angew. Chem., Int. Ed. Engl.*, 1991, **30**, 34; (b) Special issue on polyoxometalates, *Chem. Rev.*, 1998, **98**, 1; (c) D. L. Long, R. Tsunashima and L. Cronin, *Angew. Chem., Int. Ed.*, 2010, **49**, 1736.
6 (a) H. Li, S. Pang, X. Feng, K. Müllen and C. Bubeck, *Chem. Commun.*, 2010, **46**, 6243; (b) D. Zhou and B. Han, *Adv. Funct. Mater.*, 2010, **20**, 2717; (c) R. Liu, S. Li, X. Yu, G. Zhang, S. Zhang, J. Yao, B. Keita, L. Nadjo and L. Zhi, *Small*, 2012, **8**, 1398.
7 (a) W. Bu, H. Fan, L. Wu, X. Hou, C. Hu, G. Zhang and X. Zhang, *Langmuir*, 2002, **18**, 6398; (b) W. Bu, H. Li, H. Sun, S. Yin and L. Wu, *J. Am. Chem. Soc.*, 2005, **127**, 8016; (c) H. Sun, H. Li, W. Bu, M. Xu and L. Wu, *J. Phys. Chem. B*, 2006, **110**, 24847; (d) M. Xu, H. Li, L. Zhang, Y. Wang, Y. Yuan, J. Zhang and L. Wu, *Langmuir*, 2012, **28**, 14624.
8 W. S. Hummers and R. E. Offeman, *J. Am. Chem. Soc.*, 1958, **80**, 1339.
9 (a) V. A. Sinani, M. K. Gheith, A. A. Yaroslavov, A. A. Rakhnyanskaya, K. Sun, A. A. Mamedov, J. P. Wicksted and N. A. Kotov, *J. Am. Chem. Soc.*, 2005, **127**, 3463; (b) T. Zhang, P. Liu, C. Sheng, Y. Duan and J. Zhang, *Chem. Commun.*, 2014, **50**, 2889.
10 D. Volkmer, A. D. Chesne, D. G. Kurth, H. Schnablegger, P. Lehmann, M. J. Koop and A. Müller, *J. Am. Chem. Soc.*, 2000, **122**, 1995.
11 (a) S. Wen, W. Guan, J. Wang, Z. Lang, L. Yan and Z. Su, *Dalton Trans.*, 2012, **41**, 4602; (b) J. P. Tessonnier, S. Goubert-Renaudin, S. Alia, Y. Yan and M. A. Barteau, *Langmuir*, 2013, **29**, 393; (c) Wang S, Li H, Li S, Liu F, Wu D, Feng X and L. Wu, *Chem. Eur. J.*, 2013, **19**, 10895.
12 W. Bu, H. Li, W. Li, L. Wu, C. Zhai and Y. Wu, *J. Phys. Chem. B*, 2004, **108**, 12776.
13 D. Li, M. B. Müller, S. Gilje, R. B. Kaner and G. G. Wallace, *Nat. Nanotechnol.*, 2008, **3**, 101.